

Microstructured platforms to study nanotube-mediated long-distance cell-to-cell connections

Marcus P. Abel

Department of New Materials and Biosystems, Max-Planck Institute for Metals Research, Heisenbergstr. 3, D-70569 Stuttgart, Germany and Department of Biophysical Chemistry, University of Heidelberg, INF 253, D-69120 Heidelberg, Germany

Sigrid R. Riese

Department of New Materials and Biosystems, Max-Planck Institute for Metals Research, Heisenbergstr. 3, D-70569 Stuttgart, Germany; Department of Biophysical Chemistry, University of Heidelberg, INF 253, D-69120 Heidelberg, Germany; and Interdisciplinary Center of Neuroscience (IZN), Institute of Neurobiology, University of Heidelberg, INF 364, Heidelberg 69120, Germany

Oliver Schlicker

Leica Microsystems CMS GmbH, Ernst-Leitz-Straße 17-37, 35578 Wetzlar, Germany and Interdisciplinary Center of Neuroscience (IZN), Institute of Neurobiology, University of Heidelberg, INF 364, Heidelberg 69120, Germany

Nickolay V. Bukoreshtliev

Department of Biomedicine, University of Bergen, Jonas Lies vei 91, N-5009 Bergen, Norway and Interdisciplinary Center of Neuroscience (IZN), Institute of Neurobiology, University of Heidelberg, INF 364, Heidelberg 69120, Germany

Hans-Hermann Gerdes

Department of Biomedicine, University of Bergen, Jonas Lies vei 91, N-5009 Bergen, Norway and Interdisciplinary Center of Neuroscience (IZN), Institute of Neurobiology, University of Heidelberg, INF 364, Heidelberg 69120, Germany

Joachim P. Spatz

Department of New Materials and Biosystems, Max-Planck Institute for Metals Research, Heisenbergstr. 3, D-70569 Stuttgart, Germany and Department of Biophysical Chemistry, University of Heidelberg, INF 253, D-69120 Heidelberg, Germany

Amin Rustom^{a)}

Department of New Materials and Biosystems, Max-Planck Institute for Metals Research, Heisenbergstr. 3, D-70569 Stuttgart, Germany; Department of Biophysical Chemistry, University of Heidelberg, INF 253, D-69120 Heidelberg, Germany; and Interdisciplinary Center of Neuroscience (IZN), Institute of Neurobiology, University of Heidelberg, INF 364, Heidelberg 69120, Germany

(Received 27 January 2011; accepted 28 February 2011; published 18 March 2011)

Recently, numerous innovative approaches have attempted to overcome the shortcomings of standard tissue culturing by providing custom-tailored substrates with superior features. In particular, tunable surface chemistry and topographical micro- and nanostructuring have been highlighted as potent effectors to control cell behavior. Apart from tissue engineering and the development of biosensors and diagnostic assays, the need for custom-tailored platform systems is accentuated by a variety of complex and poorly characterized biological processes. One of these processes is cell-to-cell communication mediated by tunneling nanotubes (TNTs), the reliable statistical analysis of which is consistently hampered by critical dependencies on various experimental factors, such as cell singularization, spacing, and alignment. Here, the authors developed a microstructured platform based on a combination of controlled surface chemistry along with topographic parameters, which permits the controllable attachment of different cell types to complementary patterns of cell attracting/nonattracting surface domains and—as a consequence—represents a standardized analysis tool to approach a wide range of biological questions. Apart from the technical complementation of mainstream applications, the developed surfaces could successfully be used to statistically determine TNT-based intercellular connection processes as they are occurring in standard as well as primary cell cultures. © 2011 American Vacuum Society. [DOI: 10.1116/1.3567416]

I. INTRODUCTION

In addition to the development of biosensors and diagnostic assays, the control of substrate surface features has turned out to be of pivotal importance for the analysis of eukaryotic

cell culture systems and their growth characteristics. Over the past years, diverse physicochemical parameters, such as surface topography¹⁻³ and chemistry,⁴⁻⁶ have been highlighted as potent effectors to manipulate the behavior of cells on varying substrates. To date scientists can draw on a large variety of surface engineering approaches that provide the

^{a)}Electronic mail: rustom@nbio.uni-heidelberg.de

necessary tools in order to cope with an increasing range of complex biotechnological applications.

Most of the methodologies reported rely on the handling of extracellular matrix (ECM) constituents such as laminin, collagen, and fibronectin, which—unlike unspecific adhesion molecules—provide specific receptor-mediated cell binding, as it occurs in the *in vivo* situation. “Short” peptide sequences from respective proteins are being explored as alternatives to long protein chains, which fold randomly upon surface adsorption, causing active protein domains to be sterically unavailable. One example is the IKVAV peptide, which represents the main cell-binding domain of the α -chain of laminin⁷ and which was shown to promote rapid and stable cell adhesion of “neuronlike” pheochromocytoma PC12 cells⁸ as well as neuronal networks *in vitro*.⁹ Other approaches are based on the use of adhesive molecules, e.g., the cationic surfactant poly-L-lysine or different alkanethiols. In the latter case, for instance, methyl and carboxylic acid-terminated monolayers of alkanethiols on gold have been used to modulate surface wettability and thereby the behavior of murine 3T3 fibroblasts.¹⁰

Along with the formation of self-assembling monolayers (SAMs), the controlled application of molecules to surfaces is accomplished by various methods, including microcontact printing technology.¹¹ For example, microscale patterns of deposited polylysine-conjugated laminin have been used to guide neuron attachment and axon outgrowth.¹² Neurons have been enticed to grow on microelectrode arrays (MEAs) using poly-L-lysine lines, printed in close proximity to the contact elements.¹³ Photolithographic methods are also commonly used, as demonstrated by, e.g., the generation of active patterns of ECM proteins, prepared by UV photolithography, which facilitated guided outgrowth and bifurcation of neurites from leech neurons.¹⁴

In addition or as an alternative to chemical surface structuring, controlled modification of the micro- and/or nanotopography of the substrate is used to elicit controlled cellular responses. Also here, a multitude of techniques, including electron beam or photolithography in combination with reactive ion etching,¹⁻³ has been employed in order to establish iso- or anisotropic topology changes. These changes include “simple” modifications, starting from controlled surface roughness to the generation of grooves and ridges, as well as the production of “complex” surface patterns such as cylindrical fibers and/or pillar structures.³ As an example, the influence of surface roughness on the adhesion and viability of neural cells has been demonstrated by following the outgrowth of growth cones and filopodia on silicon wafers of differing nanoscale topography created by hydrofluoric acid etching.¹⁵ Other studies report how the guiding of individual cells of neuronal networks to the electrodes of MEAs was achieved by covering the electrode surfaces with carbon nanotubes generated by chemical vapor deposition.¹⁶

In order to realize complementary patterns of cell attracting and repellent surface regions, many of the described technologies rely on the application of cell adhesion inhibitors, such as polar and uncharged polyethylene glycol (PEG)

derivatives. Hydrophilic PEG surfaces are nonfouling and efficiently resist attachment of proteins and cells by exploiting stable surface hydration.¹⁷ However, respective passivating and patterning strategies—in particular when “isolating” cell individuals from each other—may have substantial implications for complex and poorly characterized intercellular communication processes, such as tunneling nanotube (TNT) mediated network formation.

TNTs were initially characterized as thin intercellular membrane channels, tensed between cultivated PC12 cells at their nearest distance and without contact to the substratum, displaying diameters from 50 to 200 nm and lengths of up to several cell diameters.¹⁸ The structures with their remarkable architecture were shown to mediate membrane continuity, to contain a F-actin and/or microtubule backbone, and to facilitate the intercellular transmission of various cellular components—including organelles as well as plasma membrane constituents.^{19,20} Above all, they were proposed to be involved in different physiological as well as pathological processes of medical interest, including viral infections,^{20,21} cancer,^{20,21} and—recently—degenerative brain disorders.²² However, the precise quantitative examination of TNT-related processes has turned out to be difficult because of (i) their pronounced sensitivity, (ii) their peculiar architecture requiring sophisticated experimental approaches, and (iii) the critical dependence on spacing, density, and singularization of respective cell systems.²³ Further complications arise from observations indicating that the occurrence of TNTs can be (i) transient, (ii) dependent on age, condition, and developmental stage of the analyzed cell system, and (iii) of heterogeneous character, i.e., occurring between cells of different origins and locations.²³ These considerations support the view that the quantitative determination of TNT-related parameters—or that of congeneric biological questions—can benefit from standardized and precisely controllable growth conditions, as provided by the described surface structuring technologies.

Here we present a novel platform system consisting of biofunctionalized gold disk microarrays which facilitate ordered cellular arrangements along with improved cell singularization. The system is based on a combination of controlled surface chemistry and topography resulting in complementary patterns of cell attracting/nonattracting surface domains. It, thus, represents a standardized and sensitive analysis tool to approach numerous biological questions—also in technical complementation of established methodologies. To highlight potential fields of application, we employed the microarrays to quantitatively determine TNT-based intercellular communication processes occurring in standard as well as primary cell cultures.

II. EXPERIMENT

A. Generation and characterization of micropatterned substrates

1. Photolithography

Microstructured surfaces were produced using standard lithographic techniques: glass cover slips (24 × 24 mm²,

Carl Roth GmbH, Karlsruhe, Germany) were coated with positive photoresist AR-P 5350 (Allresist GmbH, Strausberg, Germany) and overlaid with a chromium mask written on a maskwriter (DWL-66; Heidelberg Instruments Mikrotechnik GmbH, Heidelberg, Germany), performed on a mask aligner (MJB-3; Karl Süss MicroTec Lithography GmbH, Garching, Germany). After exposure to the mercury lamp, the photoresist was solubilized in alkaline developer AR300-35 (Allresist GmbH). The mask was removed, leaving photoresist-free holes on the blocked glass surface. Cover slips were sputtered with 5 nm titanium and 50 nm gold by a sputter coater (MED020; Bal-Tec GmbH, Witten, Germany) followed by a “lift-off” procedure with acetone p.a. and dimethylformamide p.a. (Merck KGaA, Darmstadt, Germany).

2. Biofunctionalization of gold microstructures

Microstructured cover slips were cleaned for 5 min hydrogen plasma and incubated for at least 12 h at 4 °C in 40 μ M solutions (50 μ M) of one of the following ligands: (1) IKVAV peptide (here a 19-amino acid peptide corresponding to residues 2091–2108 of the laminin α -chain, plus an N-terminal cysteine; Bachem Distribution Services GmbH, Weil am Rhein, Germany) solved in phosphate buffer (PB) buffer; (2) 11-mercaptoundecanoic acid (Sigma-Aldrich, Taufkirchen, Germany); or (3) 10-aminodecane-1-thiol solution (kindly provided by Fritz), both solved in phosphate buffered saline (PBS). After incubation, samples were rinsed three times with PB buffer or PBS on a shaker. Covalent binding of ligands to gold microstructures is expected based on their covalent binding to nonstructured gold crystals but not to silica crystals, as confirmed by quartz crystal microbalance (QCM).

3. QCM measurements

Measurements were performed using a Q-Sense E4 system (Q-Sense, Gothenburg, Sweden) as previously described.²⁴ The system was operated in flow mode with a time resolution of <1 s. Sample solutions (10 μ M ligand in PB or PBS buffer) were continuously delivered (flow rate: 60 μ l/min) to the measurement chamber by means of a peristaltic pump (ISM597D; Ismatec, Zürich, Switzerland). To switch between sample liquids, the flow was interrupted for a few seconds without disturbing the QCM signal. Prior to functionalization, silica and gold-coated QCM sensors (Q-Sense, Gothenburg, Sweden) were cleaned by immersion in a 2% sodium dodecyl sulfate solution for 30 min, rinsing with Milli-Q water, blow drying with a stream of nitrogen, and exposing to oxygen plasma (0.4 mbar, 150 W) (100-E Plasma System; TePla, Feldkirchen, Germany) for 30 min. Cleaned substrates were stored in air and were again exposed (5 min) to oxygen plasma prior to use.

B. Cell culture and transfection

PC12 cells (rat pheochromocytoma cells, clone 251)²⁵ were cultured in Dulbecco's Modified Eagle Medium (DMEM) supplemented with 10% fetal calf serum and 5%

horse serum according standard procedures. For transfection experiments, the following cDNA construct was used: vesicular stomatitis virus glycoprotein-enhanced cyan fluorescent protein (kindly provided by Keller). Electroporation was performed as described²⁶ and cells were replated on microstructured arrays 24 h after transfection. Primary hippocampal neurons and astrocytes from fetal E18 Wistar rats were prepared as previously described.²⁷ Prior to microscopic analysis, the cells were plated on biofunctionalized gold disk arrays at 5×10^5 cells/surface, i.e., at a ratio of one cell per gold disk. Whereas neurons were plated directly after the preparation, astrocytes were first cultured for 7, 14, or 21 days in cell culture flasks (Nunc GmbH & Co. KG, Wiesbaden, Germany) coated with poly-L-lysine. The cell culture medium consisted of modified neuronal minimum essential medium with B27 neurobasal supplement and penicillin-streptomycin-neomycin antibiotic mix (Invitrogen GmbH, Darmstadt, Germany) and was changed after 2, 3, and 8 days. For coculturing experiments, astrocytes and neurons were coplated at 5×10^5 cells/surface for 4 h at a ratio of 1:2. In order to be able to distinguish unequivocally between both cell types, astrocytes were fluorescently labeled with DiI and neurons with CellTracker™ blue (see below). During all steps, particular attention was paid to the singularization of cells by thorough resuspension.

C. Microscopy and dye staining

1. High resolution scanning electron microscopy

For scanning electron microscopy (SEM), cells were carefully fixed with 2.5% glutaraldehyde and 0.1M sodium cacodylate (pH 7.4), dehydrated in a graded series of ethanol, and critically point dried using CO₂. Afterward, a carbon layer was sputtered (Sputter-Coater MED020, Bal-Tec GmbH) on the samples. Samples were imaged by a ZEISS LEO 1530 in-lens field emission scanning electron microscope (Carl Zeiss NTS GmbH, Oberkochen, Germany).

2. Bright field and fluorescence microscopy

Bright field as well as fluorescence microscopy was performed with a monochromator-based imaging system (T.I.L.L. Photonics GmbH, Martinsried, Germany) mounted on an Olympus IX70 microscope (Olympus Optical Co. Europa GmbH, Hamburg) equipped with 100 \times PlanApo NA 1.40 or 40 \times PlanApo NA 0.95 objectives (Olympus Optical Co. Europe GmbH) and a triple-band filter set DAPI/FITC/TRITC F61-020 (AHF Analysentechnik AG, Tübingen, Germany). For three-dimensional (3D) analysis, a piezo-z-stepper (E-662; Physik Instrumente GmbH & Co., Karlsruhe, Germany) controlled by the TILLVISION System was used. The microscope was surrounded by a 37 °C heating control device and equipped with a 5% CO₂ supply (Live Imaging Services, Olten, Switzerland). Pictures were taken by a charge-coupled device camera (IMAGO-QE; T.I.L.L. Photonics GmbH, Martinsried, Germany) controlled by TILLVISION software (Version 4.01; T.I.L.L. Photonics GmbH).

3. Spinning disk microscopy

Confocal microscopy was performed on a Perkin Elmer Ultraview system mounted on a Nikon TE 2000E inverted microscope with Nanoscan z-device, equipped with Nikon Plan Apo VC 100 \times NA 1.4 or VC 60 \times NA 1.4 oil-immersion planapochromatic objectives (Nikon GmbH, Düsseldorf, Germany) and surrounded by a heating chamber (Tokai Hit Microscope Incubation System; Tokai Hit Co., Ltd., Japan). The system uses a Perkin Elmer spinning disk confocal ERS-FRET Unit (laser lines: 405, 488, and 568 nm) in combination with the following filter sets: CFP-YFP, GFP-mRFP, or CFP-mRFP (Perkin Elmer Inc., MA). Pictures were taken by a 30 Hz charge-coupled device camera (resolution: 1024 \times 1024 pixel) (EM-CCD; Hamamatsu Photonics Deutschland GmbH, Herrsching am Ammersee, Germany). For 3D analysis, a piezo z-stepper (Perkin Elmer, Inc.) was used. Camera and z-stepper were controlled by the ULTRAVIEW ERS software system. Images were processed with the Perkin Elmer Volocity acquisition software (Version 5.21).

4. Atomic force microscopy

The atomic force microscopy (AFM) system contained a Nano-Wizard I AFM with a CellHesion module (JPK Instruments AG, Berlin, Germany) mounted on an AxioVert 200 microscope (Carl Zeiss, Göttingen, Germany). The AFM was placed in a CO₂ incubator box controlled by an EMBL GPI68 IV custom-tailored system. Data were analyzed and force curves were corrected for cantilever drift and different support positions via MATLAB software (MathWorks, Natick, USA). The cantilevers (Veeco NanoProbe NP-S; Veeco, Camarillo, USA) were used in standard intermittent contact mode operation in PBS. For AFM studies, modified petri dishes were used as described (see D. Microinjection).

5. Dye staining

For plasma membrane staining, WGA Alexa Fluor[®] 488 conjugate at a concentration of 1 mg/ml (Invitrogen GmbH) was added directly to the culture medium (1:300). Vybrant[™] DiI cell labeling solution (Molecular Probes, Invitrogen GmbH) and CellTracker[™] blue solution (Invitrogen GmbH; 20 μ M final concentration) were used for labeling cells in suspension according to the supplier's instructions.

D. Microinjection

Microstructured arrays biofunctionalized with IKVAV peptid were prepared as described and glued to a 1.4 cm opening, drilled in a petri dish. 5×10^5 PC12 cells were plated on the surfaces. After 1 h of incubation, selected cells were injected with Cytochrome C solution [10 μ l (12.5 mg/ml) Cytochrome C dissolved in 3 μ l TRITC-dextran; Sigma-Aldrich] and loaded into a microinjection needle, using a micromanipulation system (FemtoJet[®]; Eppendorf AG, Hamburg, Germany) mounted on a conventional fluorescence microscope (Olympus IX70; Olympus Optical Co. Europa GmbH). Pictures were taken at given time points.

E. Flow cell analysis

A custom-tailored flow cell comprised of a teflon-based body (external diameter of 5.4 cm and bore diameter of 2.5 cm) and a cover plate consisting of acrylic glass was constructed. Microstructured and biofunctionalized surfaces were glued to the cutout at the bottom side of the base body. For the experiments, 3.5×10^5 cells were plated in the cell chamber and incubated for 1–3 h at 37 °C and 5% CO₂. The chamber was mounted on the stage of the spinning disk microscope. Cell culture medium flow was guided by a tubing system connected to the teflon body and regulated via plugs at the junctions. The flow speed was controlled by a syringe pump [Harvard Spritzenpumpe 11 (RS-232); Harvard Apparatus, MA] connected to the tubing system. Flow rates of 0.25, 0.5, and 0.75 ml/min were applied and pictures taken and processed as described.

F. Statistical analyses

All statistical data provided represent the mean of ten independent experiments. In each experiment at least 15 randomly chosen microscopic areas (each covering no fewer than 20 cells) were analyzed. Error bars represent the standard deviation of the mean.

III. RESULTS AND DISCUSSION

A. Preparation and application of microstructured gold disk arrays

The general procedure used for the fabrication of micro-patterned surfaces consisting of regular arrays of circular gold disks and their subsequent biochemical functionalization is outlined in Figs. 1(A)–1(C). In brief, according to standard lithographic techniques, the positive photoresist was spin coated to glass slides, irradiated through a chromium mask by exposure to UV light, followed by the developing process and sputtering of a basic layer of titanium and a top layer of gold to the surfaces. A lift-off process revealed the final disk arrays [Fig. 1(A)]. Surface parameters were selected to match an average cell diameter of 13 μ m with regard to the PC12 model cell system in focus of this study. Because gold disks can—in dependency on the thickness of the sputtered metal layers—be opaque, their diameter was set to 10 μ m which causes attached cells to marginally overlap in order to ease the light microscopic visualization of their peripherals. The bearing corner radius was set to 20 μ m in order to avoid contact of individual cells with more than one gold disk. The disk pattern was arranged in a regularly “quadratic” configuration to be able to monitor distance dependent variations, provoked by permitting orthogonal as well as diagonal cell interactions.

The analysis of respective surfaces by scanning electron microscopy (see Sec. II) showed that gold disk arrays were homogeneous and without visible defects [Fig. 1(B)], proving that the technique can be used to realize the fast preparation of large surface areas and thus providing advantages in comparison to other techniques, such as, e.g., e-beam lithography. Due to the use of a negative pitch angle of the photo-

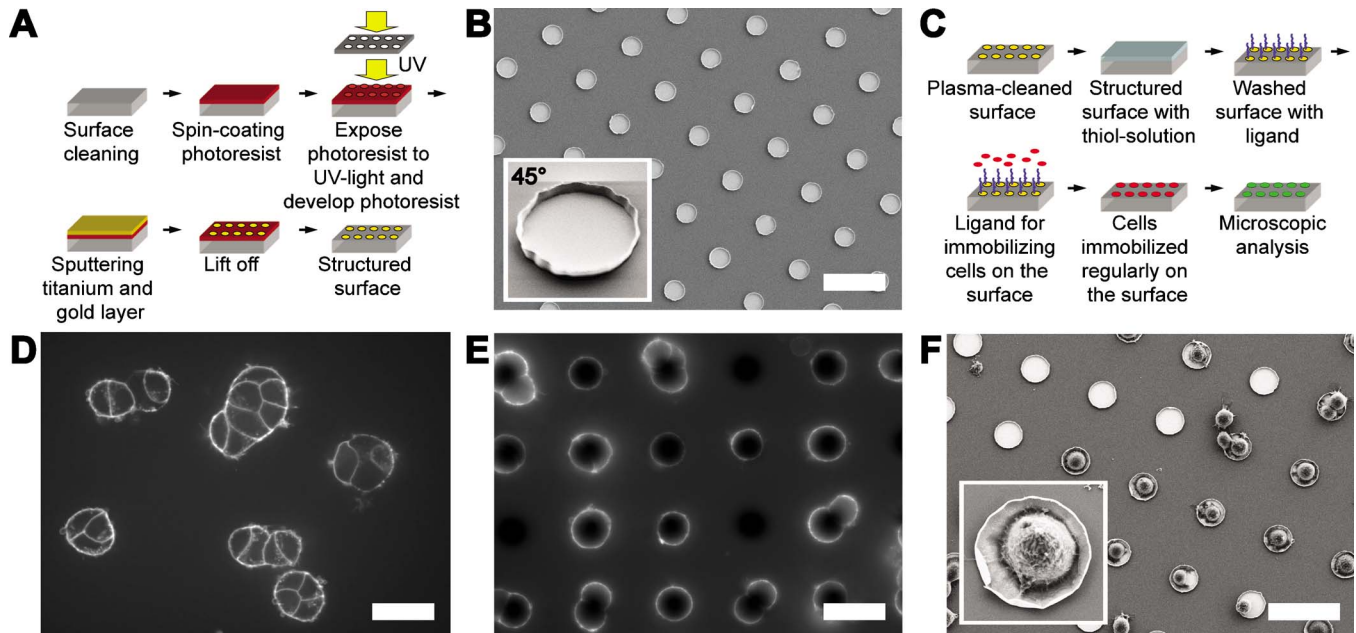


FIG. 1. (Color online) Preparation and application of microstructured gold disk arrays. Schematic illustrations of the principle of surface structuring and biofunctionalization are shown in (A) and (C), respectively. SEM images of the surfaces prior to functionalization are shown in (B). The inlay in (B) shows a magnified area in 45° perspective as indicated and reveals the brimlike edge of the gold disks. The comparison of WGA stained PC12 cells grown on conventional glass surfaces (D) and biofunctionalized substrates (E) and (F) demonstrates improved cell singularization and regular arrangement as documented by fluorescence (D) and (E) as well as scanning electron microscopy (F). Scale bars: 30 μm .

resist in combination with an adapted sputtering process (see Sec. II), it was possible to realize a brimlike edge of the gold disks with a height of approximately 250 nm, as measured by atomic force²⁸ and scanning electron microscopy [Fig. 1(B), inlay 45°]. This “fencelike” topographic feature seems to help constraining the lateral movements of rounded cells prior to cell attachment and spreading as they are occurring right after the plating process and may represent an advantage over planar surfaces generated by primarily “two-dimensional” patterning techniques.

The biofunctionalization of microstructured arrays was realized by the application of SAMs of adhesion promoting molecules, which covalently bind to the gold disk surfaces via functional thiol groups [Fig. 1(C)]. After plasma treatment to remove organic impurities on the glass and to further reduce its attraction for cells and molecules, three different ligands were applied (see Sec. II). In order to provide receptor specific binding as well as unspecific ionic interactions, we either used IKVAV peptide or two differently charged alkanethiols, 11-mercaptoundecanoic acid and 10-aminodecane-1-thiol. Covalent binding of thiolated ligands to gold surfaces was evaluated by QCM measurements.²⁸ Molecules physisorbed on the glass surface between the gold disks were removed by a series of washing steps. The combined effect of controlled surface chemistry and microtopography was finally evaluated by comparing the growth characteristics of PC12 cells cultivated on structured and nonstructured surfaces [Figs. 1(D)–1(F)]. Cells were plated on conventional glass cover slips or biofunctionalized gold disk arrays and analyzed 2 h later by fluorescence as well as scanning electron microscopy (see Sec. II). In contrast to

cells grown on glass substrates, which tend to form large clusters and display disordered growth patterns [Fig. 1(D)], the use of microstructured arrays functionalized with IKVAV peptide strongly increased cellular order [Figs. 1(E) and 1(F)]. Cells appeared nicely singularized and arranged in congruence with the predefined gold disk patterns. Only occasionally small clusters of two to three cells were attached to one disk, most likely due to an imperfect separation process or—at later time points—cell divisions (see below). The use of 11-mercaptoundecanoic acid as well as 10-aminodecane-1-thiol as ligands led to cell clustering as observed on standard glass substrates,²⁸ indicating that the non-specific adhesion forces provided by these molecules are too weak to attract cells to the disk surface. Interestingly, the use of positively charged 10-aminodecane-1-thiol resulted in strongly increased affinity of hippocampal cells to the gold disks (see below). These findings clearly document that the biofunctionalization strategy has to be carefully adapted to the specific requirements of the respective cell system. Cells strictly kept their positions on the IKVAV-functionalized gold disks even during longer observation periods, i.e., no “jumps” between the disks were observable. They showed no apparent morphological changes—apart from the “shape” change induced by the predefined patterning—and still divided attached to the gold disks, implementing that after prolonged time periods, larger cell clusters are formed. We found no indication for an increased apoptosis rate, as observed for, e.g., capillary endothelial cells restricted to fibronectin coated islands with a diameter of 10 μm .²⁹

In supplemental experiments, the microstructured arrays functionalized with IKVAV peptide were successfully used in

complementation with different standard methodologies in order to address several PC12 cell related topics. These include microinjection experiments utilizing apoptosis inducing molecules, whereby, when compared to the standard application on conventional surfaces, (i) accessibility and subsequent analysis of individual cells was strongly facilitated and (ii) the movement of cells was virtually disabled, maintaining the initial cell configuration even during long-term observations.²⁸ Furthermore, in experiments subtle morphological changes induced by the transient expression of viral transmembrane proteins²⁸ could be monitored, which had been difficult to observe and quantitatively determine under standard cell culture conditions. In conclusion, the ability of the developed surfaces to control cell attachment and singularization combined with their broad adaptability, based on the flexibility of the gold/thiol based chemical linker system and the lithography process, make these arrays an ideal analysis platform for a wide range of applications.

B. Ordered growth of hippocampal cocultures

To evaluate the usefulness of the designed microstructured platform system for challenging primary cell cultures, we next analyzed the growth characteristics of cocultures of neurons and astrocytes isolated from fetal rat hippocampus. Cells were prepared and fluorescently labeled where required according standard procedures (see Sec. II) and plated on biofunctionalized gold disk arrays as described. In order to achieve fast and selective cell attachment, disk surfaces were functionalized with 10-aminodecane-1-thiol since the use of IKVAV peptide or 11-mercaptoundecanoic acid leads to strong cell clustering, affecting either one or both of the coplated cell types.²⁸ Employing bright field as well as scanning electron microscopy (see Sec. II), we could show that neurons as well as astrocytes attached selectively to the gold disks [Fig. 2(A)]. Whereas neurons with their relatively small cell bodies attached selectively to one disk, larger astrocytes were able to span several disks [Fig. 2(B)]. Remarkably, the outgrowth of cellular protrusions—in particular neurites—followed exclusively paths determined by the disk pattern, resulting in ordered cellular assemblies [Fig. 2(C)]. This observation agrees with an increasing number of studies that employed various chemical and/or topographical surface modifications to control the outgrowth of, e.g., neurites in neuronal cultures.^{12,14} Apart from the general advantages of an increased order parameter, it is important to note that the tight association of neuronal cells or subcellular domains, such as, e.g., defined segments of axons or dendrites, to individually accessible and electrically conducting metal surfaces could—upon the addition of isolated conducting paths—represent a further step toward the development of advanced bioelectronic devices, such as biosensors and neuronal networks. Along with recent endeavors to develop semiconducting silicon biointerfaces,³⁰ such technologies may, in the future, revolutionize, e.g., present MEA technology.

Staining of cellular plasma membranes with labeled WGA (see Sec. II) followed by high-resolution 3D fluorescence

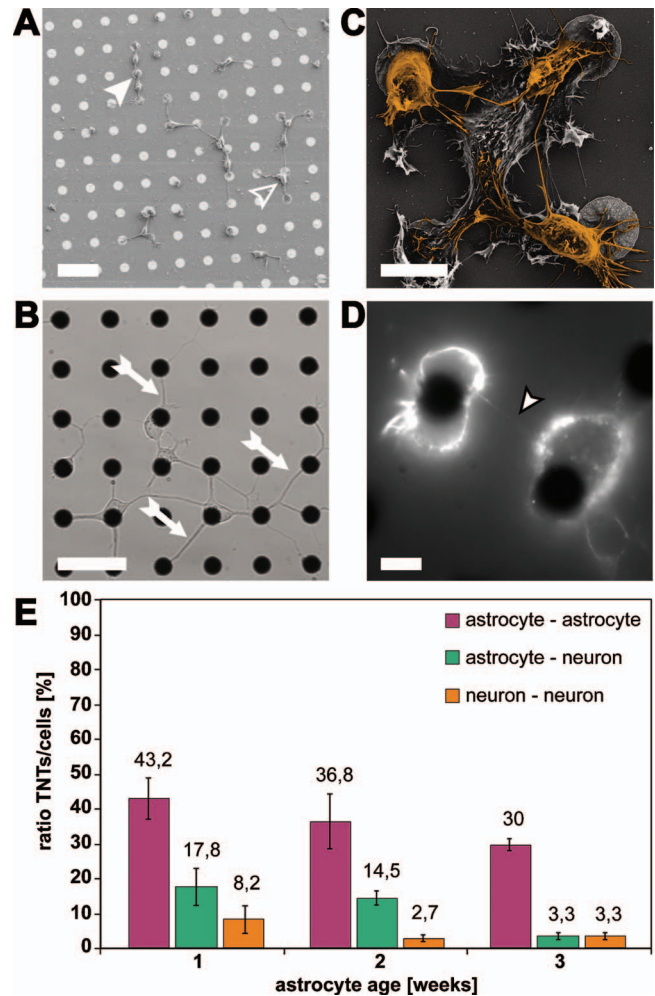


FIG. 2. (Color) Ordered growth of hippocampal cocultures on micropatterned surfaces reveals prospective TNT structures. Hippocampal neurons and astrocytes of varying ages were prepared and coplated on micropatterned surfaces as described. Cells were analyzed by scanning electron (A) and (C), bright field (B), and fluorescence microscopy (D) 4 h after plating. Please note that neurons (closed arrowhead) as well as astrocytes (open arrowhead) attach selectively to gold disks (A) and their protrusions (arrows) follow exclusively paths determined by the microstructures (B). Whereas neuronal cell bodies (yellow) attach to single disks, larger astrocytes are able to span several gold structures (C). 3D fluorescence microscopy of WGA stained cocultures revealed prospective TNT structures spanned between individual cells at their nearest distance and without contact to the substrate (black bordered arrowhead)—here between two astrocytes (D). A comprehensive statistical analysis yielded cell type and age dependent differences of the TNT number (E). Scale bars: (A) and (B) 40 μm ; (C) and (D) 10 μm .

microscopy revealed that cocultured neurons and astrocytes were frequently interconnected by thin membrane tubes [Fig. 2(D)], displaying the same dimensions and architectural characteristics as previously described for TNT structures detected in various cell culture systems (see above). Due to the increased order parameter induced by disk association, the structures—suspended above the substratum—were clearly distinguishable from other cellular extensions, like neurites or filopodia. This was documented by precise analysis of the corresponding 3D image information. A quantitative analysis revealed that the largest fraction of the TNT resembling

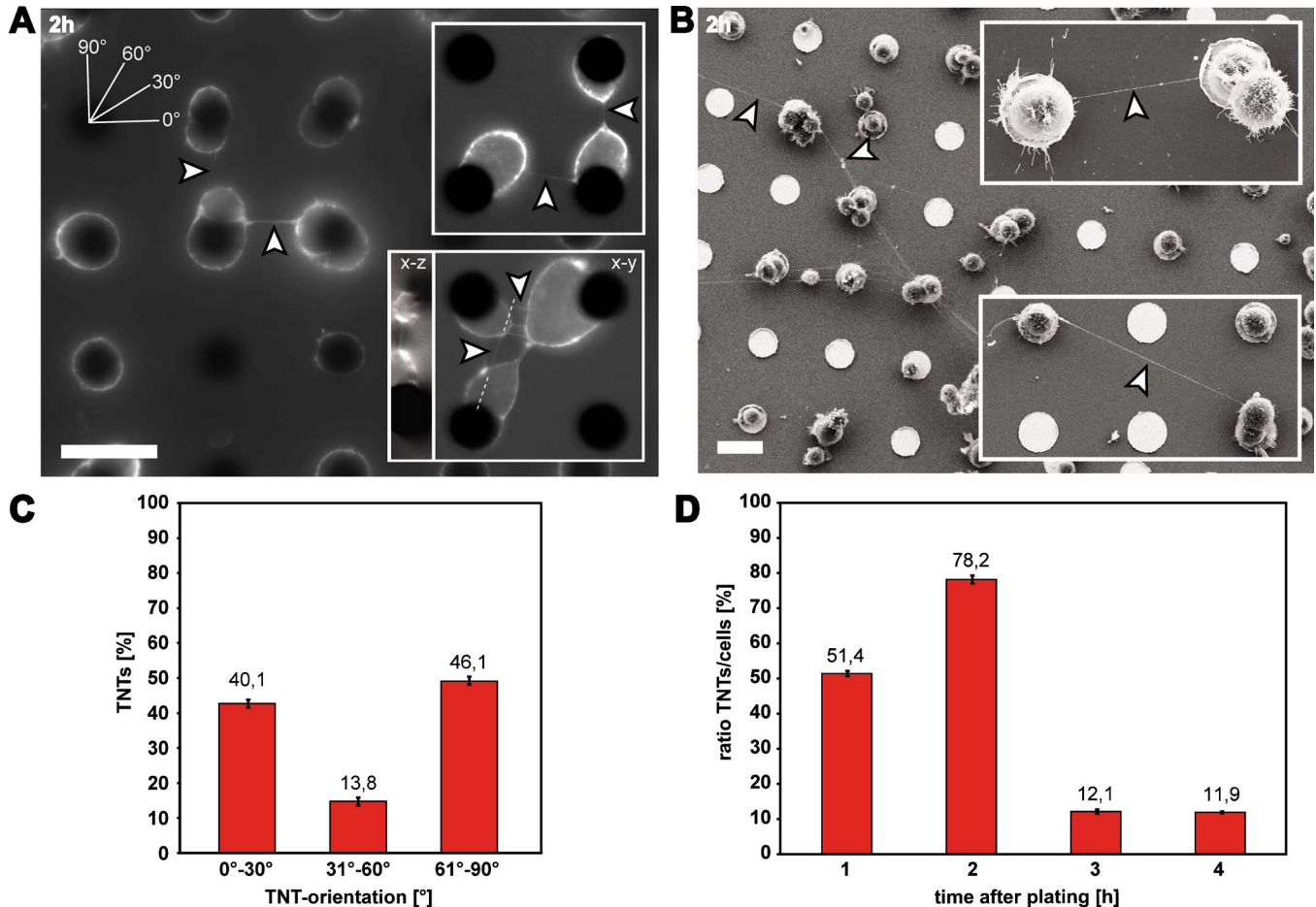


Fig. 3. (Color online) Quantitative analysis of TNT-based network formation on micropatterned surfaces reveals distance dependency of TNT formation. PC12 cells were grown on biofunctionalized gold disk arrays and analyzed by high-resolution 3D fluorescence (A) as well as scanning electron microscopy (B) at different time points as described. Prior to fluorescence microscopy, cell membranes were stained with fluorescently labeled WGA. TNT structures are marked by arrowheads. Frequently, the formation of small (A, inlays) or extended TNT networks (B) could be observed. 3D analysis revealed that TNTs formed between cells at their nearest distance have no contact to the substrate and are aligned mostly parallel to the surface (A, bottom inlay, X-Z). The dotted lines represent the cutting plane for the shown X-Z representation. The quantitative analysis of the angle of TNT alignment with respect to the disk pattern revealed that the diagonal orientation (31°–60°) is less frequent than the orthogonal ones (C). Evaluation of the overall TNT number at different time points after cell plating revealed a maximum at 2 h after plating (D). Bars: 20 μm .

structures was found among astrocytes, the second largest fraction was detected between neurons and astrocytes, and the lowest but still significant number was determined to connect neurons to one another [Fig. 2(E)]. These observations are in close connection with previous studies, showing a TNT-dependent transfer of, e.g., prion proteins between cells of the catecholaminergic mouse neuronal cell line CAD as well as from bone marrow derived dendritic cells to primary neurons,³¹ thus, further strengthening the concept of a complex and relevant participation of the respective membrane channels in *in vivo* brain functioning—particularly during intercellular exchange and communication processes. Additional support for this theory comes from a recent study proposing TNT-dependent exchange of mitochondria between cortical rat astrocytes or glioblastoma cells.²² An interesting observation during our study was that—while the cell type-dependent distribution widely persisted—the overall number of TNT resembling structures decreased by approximately one-third per week with progressing astrocyte

age [Fig. 2(E)]. A finding which is in accordance with the reduced TNT number was observed for PC12 cell cultures of increasing passage numbers.³² Taken together, our results may provide first indications of cell type-dependent as well as development or age-related influences on brain related TNT action, which will be the focus of future experiments.

C. Analysis of TNT-based network formation

To further investigate the applicability of the microstructured platform system with respect to membrane tube-mediated communication processes, we proceeded by analyzing PC12 cells regarding their TNT-formation capabilities. Cells were plated on functionalized disk arrays and analyzed 2 h later by 3D fluorescence and high-resolution scanning electron microscopy as described. As already shown, cells appeared nicely singularized and attached selectively to the gold disks [Figs. 3(A) and 3(B)]. TNT structures tensed at their nearest distance and without contact

to the substratum could be detected between them, frequently forming expanded networks which consisted of three or more individual cells. The overall length distribution of the membrane tubes showed a maximum at 4 μm ,²⁸ which correlates with previous studies based, e.g., on the computer assisted analysis of TNTs in PC12 cultures grown on conventional substrates,³³ further fuelling speculations concerning an optimal distance for membrane tube formation.³³ However, it is important to stress that throughout literature the TNT length distribution appears rather heterogeneous, particularly when comparing structures formed between different cell types. For example, most TNTs between neuronal CAD cells had an average length of around 25 μm .³¹ The observed heterogeneity is certainly amplified by the dependence of TNTs on cell morphology, culture conditions, and, especially, cell density and singularization, once more emphasizing the need of standardized platform systems. The discrepancy between the observed TNT lengths and the 20 μm bearing corner distance of the gold disks can be explained by the observation that cells on neighboring gold supports do not necessarily attach to the central region of the disks. This applies, in particular, to TNT-connected cells [Fig. 3(A), inlays] and points to drag forces mediated, e.g., by membrane tension or the cytoskeletal TNT backbone. Nevertheless, TNTs bridging larger distances of more than 50 μm between cells attached to non-neighboring disks were also frequently documented [Fig. 3(B)].

A statistical analysis of the height differences between both TNT bases, based on 3D image information [Fig. 3(A), bottom inlay, *X-Z*], revealed a strong maximum between 0.5 and 1.5 μm ²⁸ proving that most of the structures are aligned relatively parallel to the surface. This represents an additional advantage of the microarrays over standard surfaces, particularly in view of the challenging microscopic 3D TNT visualization. Interestingly, a statistical analysis of TNT alignment with respect to the disk pattern revealed that the diagonal TNT configuration (31° – 60°) was approximately one-third as frequent as the orthogonal one [Fig. 3(C)]. Together with their overall length distribution²⁸ this provides a strong and to our knowledge first indication of a distance dependency in the TNT-formation process.

Further quantitative analysis showed that the overall amount of TNTs formed on microstructured surfaces was reduced by 6%, as compared to the situation on conventional glass surfaces. This slight reduction is in excellent agreement with a recent study documenting that whereas 93% of TNTs formed between PC12 cells on standard surfaces due to filopodia interplay near the substrate, 7% were formed by the dislodgment of neighboring cells³⁴—a mechanism which is efficiently blocked by the “entrapment” of single cells on the gold disks. This indicates, in turn and along with a normal length distribution, that the main formation process of TNTs—most likely mediated by the action of filopodia—is largely unaffected by the specific properties of the microstructured surfaces, e.g., their fence-like 3D topography. The interesting question of whether TNT formation is dependent on cell-matrix interactions or occurs exclusively via cell-cell

interactions could be unambiguously answered using a passivation layer between the gold disks and will be a matter of future experiments.

The maximal amount of TNTs between cells was observed 2 h after plating, followed by an apparent decrease [Fig. 3(D)]. This result is consistent with previous studies monitoring a strong increase in the TNT number during the first 2 h after plating of PC12 cells on conventional glass surfaces.¹⁸ At longer incubation times, the TNT number stabilized at an average level [Fig. 3(D)]. Together, this clearly points to transient TNT promoting factors emerging contemporary to the plating process, i.e., a process of extensive cellular reorientation. Our results demonstrate that the biofunctionalized gold disk arrays effectively function as a sensitive and quantitative analysis system, which in future may serve as a valuable tool to study subtle effects on TNT-related properties induced, e.g., by pharmacological substances or chemical compounds, such as, e.g., methyl- β -cyclodextrin³⁵ which alters plasma membrane composition via cholesterol depletion.

D. Influence of shear stress on TNT formation

Another efficient way to influence TNTs is based on their pronounced and, particularly under standard cell culture conditions, hardly predictable sensitivity to various experimental influences, ranging from mechanical stress up to prolonged light exposure (see above). Any or all of which consistently hamper reproducible structural and functional analyses. We were therefore interested in using the developed gold disk arrays to quantitatively analyze the impact of mechanical forces on TNT formation and stability under reproducible conditions in order to gain insights into their mechanosensitive properties and—potentially—their formation process. One hour after plating, PC12 cells arranged on gold disk arrays were exposed to a constant medium flow of 0.5 ml/min in a custom-tailored flow cell setup (see Sec. II) whereby disk patterns were aligned with the flow direction [Fig. 4(A)]. 3D spinning disk microscopy revealed a strong reduction in the overall TNT number as documented by an apparent drop of the TNT/cell ratio from 78.2% to 24.2% and from 11.9% to 2.7% at 2 and 4 h after plating, respectively [Fig. 4(C)]. Whether these differences are related to varying “mechanical” susceptibilities of the TNT-formation process, which predominates 2 h after plating, or destruction of already accomplished TNT structures will remain a matter of speculation at this stage. It is important to note that more than 75% of all TNTs detected were aligned in an angle of 0° – 30° —i.e., mostly parallel—to the flow direction [Fig. 4(B)]. The smallest TNT fraction, not even 5%, was observed at an angle of 31° – 60° relative to the flow, i.e., in diagonal configuration [Fig. 4(B)]. This finding seems contradictory at first because the highest force is expected to act orthogonal (61° – 90°) to the flow. It is, however, relativized by our previous finding that under “no-flow” conditions the diagonal configuration is around one-third as frequent as the orthogonal ones (see above). That unquantifiable alterations in the flow are responsible for the observed differences

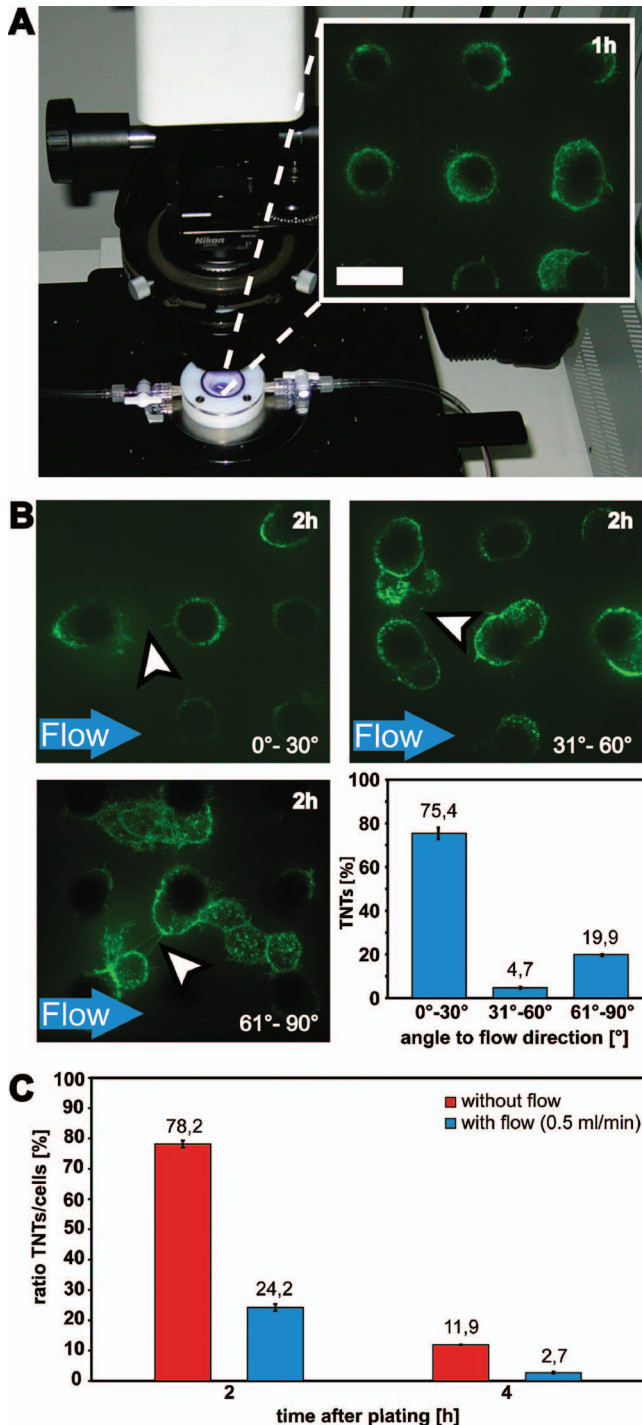


FIG. 4. (Color) Dissecting the influence of shear stress on the formation and stability of TNTs by combined flow cell analysis. PC12 cells were plated on micropatterned arrays as described and placed in a custom-tailored flow cell chamber mounted on a spinning disk confocal microscope (A). After 1 h, a constant flow rate of 0.5 ml/min was applied for additional 1 or 3 h. Thereafter, cells arranged on gold disks arrays were stained with fluorescently labeled WGA (A, inlay) and analyzed for the number and orientation of TNTs (arrowheads) by 3D fluorescence microscopy (B). Please note that the disk patterns were always aligned with the flow direction (blue arrows). A statistical evaluation shows that under flow conditions most TNTs were found at an angle of 0°–30°—i.e., mostly parallel—to the flow direction (graph in B). Along with the reduced TNT number observed between 2 and 4 h after plating [compare Fig. 3(D)], the flow induced a strong reduction of the overall TNT number (C). Scale bars: 20 μm .

seems unlikely because experimental variations in the flow rate, ranging from 0.25 up to 0.75 ml/min, evoked only minor effects.²⁸ Our findings are in analogy to previous studies that documented a decrease in TNT numbers in response to shaking the cell culture dishes^{36–38} and clearly point to the disruption of TNTs by mechanical shearing forces induced by the medium flow. Whether or not also potential soluble signaling molecules involved during TNT formation are unilaterally deflected by the continuous fluid stream remains unanswered yet.

IV. SUMMARY AND CONCLUSIONS

The developed microstructured substrates proved to be a sensitive platform system to quantitatively monitor distance and—in combination with a flow cell—also orientation-dependent aspects of TNT-mediated intercellular communication processes. Particularly with respect to the predicted physiological and pathological implications, similar technological combinations may help to unravel the influence of, e.g., soluble gradients of candidate signaling molecules on TNT network formation. Moreover, with some specific features, including fast production times, specific material composition, precise control over the positioning and immobilization of different cell types, and—in particular—the flexibility with respect to topographical as well as chemical surface patterning, the straightforward methodology described here may also assist in the development of novel high-throughput fabrication methods for inexpensive biologically suitable substrates and electrically active biosensors, having the potential to contribute to the standardized, reproducible, and quantitative analysis of a variety of biological questions.

ACKNOWLEDGMENTS

The authors would like to thank Rudolf Kern for help during microinjection experiments. The authors have to thank Hilmar Bading for infrastructure and support as well as the “Nikon Imaging Center” Heidelberg for access to the spinning disk confocal microscope. The Max Planck Society, the “NanoII” (Grant No. NMP4-LA-2009-229289) and “NanoCard” (Grant No. NMP3-SL-2009-229294) projects within the European 7th Framework Program as well as the DFG (Grant No. Ge 550/3, SFB 488) are acknowledged for financial support. The authors additionally thank Julia Ranzinger, Dimitris Missirlis, and Elisabeth Pfeilmeier for critical comments on the paper.

¹A. Curtis and C. Wilkinson, *Biomaterials* **18**, 1573 (1997).

²D. Hoffman-Kim, J. A. Mitchel, and R. V. Bellamkonda, *Annu. Rev. Biomed. Eng.* **12**, 203 (2010).

³A. S. G. Curtis and C. D. W. Wilkinson, *J. Biomater. Sci., Polym. Ed.* **9**, 1313 (1998).

⁴B. D. Ratner and S. J. Bryant, *Annu. Rev. Biomed. Eng.* **6**, 41 (2004).

⁵D. G. Castner and B. D. Ratner, *Surf. Sci.* **500**, 28 (2002).

⁶C. S. Chen, M. Mrksich, S. Huang, G. M. Whitesides, and D. E. Ingber, *Biotechnol. Prog.* **14**, 3 (1998).

⁷K. Tashiro, G. C. Sephel, B. Weeks, M. Sasaki, G. R. Martin, H. K. Kleinman, and Y. Yamada, *J. Biol. Chem.* **264**, 27 (1989).

⁸Y. Wu, Q. Zheng, J. Du, Y. Song, B. Wu, and X. Guo, *J. Huazhong Univ.*

- Sci. Technol. Med. Sci. **26**, 594 (2006).
- ⁹C. L. Klein, M. Scholl, and A. Maelicke, *J. Mater. Sci.* **10**, 12 (1999).
- ¹⁰D. A. Hutt, E. Cooper, L. Parker, G. J. Leggett, and T. L. Parker, *Langmuir* **12**, 5494 (1996).
- ¹¹D. Falconnet, G. Csucs, H. M. Grandin, and M. Textor, *Biomaterials* **27**, 3044 (2006).
- ¹²L. Kam, W. Shain, J. N. Turner, and R. Bizios, *Biomaterials* **22**, 1049 (2001).
- ¹³C. D. James *et al.*, *IEEE Trans. Biomed. Eng.* **47**, 1 (2000).
- ¹⁴P. Fromherz and H. Schaden, *Eur. J. Neurosci.* **6**, 1500 (1994).
- ¹⁵Y. W. Fan, F. Z. Cui, S. P. Hou, Q. Y. Xu, L. N. Chen, and I.-S. Lee, *J. Neurosci. Methods* **120**, 17 (2002).
- ¹⁶A. Greenbaum, S. Anava, A. Ayali, M. Shein, M. David-Pur, E. Ben-Jacob, and Y. Hanein, *J. Neurosci. Methods* **182**, 219 (2009).
- ¹⁷P. Gong and D. W. Grainger, *Methods Mol. Biol.* **381**, 59 (2007).
- ¹⁸A. Rustom, R. Saffrich, I. Markovic, P. Walther, and H. H. Gerdes, *Science* **303**, 1007 (2004).
- ¹⁹*Cell-Cell Channels*, edited by F. Baluska, D. Volkmann, and P. W. Barlow (Springer, New York, 2006), pp. 200–207.
- ²⁰S. Gurke, J. F. V. Barroso, and H. H. Gerdes, *Histochem. Cell Biol.* **129**, 539 (2008).
- ²¹J. Hurtig, D. T. Chiu, and B. Önfelt, *Wiley Interdiscip Rev Nanomed Nanobiotechnol.* **2**, 260 (2010).
- ²²L. F. Agnati, D. Guidolin, M. Guescini, S. Genedani, and K. Fuxe, *Brain Res. Rev.* **64**, 137 (2010).
- ²³A. Rustom, *Ann. N.Y. Acad. Sci.* **1178**, 129 (2009).
- ²⁴F. Hook, C. Larsson, and C. Fant, *Encyclopedia of Surface and Colloid Science* (CRC, Boca Raton, 2002), pp. 774–791.
- ²⁵L. A. Greene and A. S. Tischler, *Proc. Natl. Acad. Sci. U.S.A.* **73**, 7 (1976).
- ²⁶A. Rustom, D. Gerlich, R. Rudolf, C. Heinemann, R. Eils, and H. H. Gerdes, *BioTechniques* **28**, 4 (2000).
- ²⁷G. Banker and K. Goslin, *Nature (London)* **336**, 6195 (1988).
- ²⁸See supplementary material at <http://dx.doi.org/10.1116/1.3567416> for respective data.
- ²⁹C. S. Chen, M. Mrksich, S. Huang, G. M. Whitesides, and D. E. Ingber, *Science* **276**, 5317 (1997).
- ³⁰P. Fromherz, *ChemPhysChem* **3**, 276 (2002).
- ³¹K. Gousset *et al.*, *Nat. Cell Biol.* **11**, 328 (2009).
- ³²A. Rustom and H. H. Gerdes (unpublished).
- ³³E. Hodneland, A. Lundervold, S. Gurke, X. C. Tai, A. Rustom, and H. H. Gerdes, *Cytometry, Part A* **69**, 9 (2006).
- ³⁴N. V. Bukoreshtliev, X. Wang, E. Hodneland, S. Gurke, J. F. V. Barroso, and H. H. Gerdes, *FEBS Lett.* **583**, 9 (2009).
- ³⁵A. Rustom, M. Abel, and J. Ranzinger (unpublished).
- ³⁶S. Gurke, J. F. V. Barroso, E. Hodneland, N. V. Bukoreshtliev, O. Schlicker, and H. H. Gerdes, *Exp. Cell Res.* **314**, 3669 (2008).
- ³⁷M. Koyanagi, R. P. Brandes, J. Haendeler, A. M. Zeiher, and S. Dimmeler, *Circulation* **112**, 17 (2005).
- ³⁸S. Sowinski *et al.*, *Nat. Cell Biol.* **10**, 2 (2008).